Functional Materials 21, No.2 (2014) © 2014 — STC "Institute for Single Crystals"

Features of energy transport in $EuMgB_5O_{10}$ and EuP_3O_9 quasi-one-dimensional lattices

N.V.Kononets, V.V.Seminko, P.O.Maksimchuk, I.I.Bespalova, A.A.Masalov, Yu.V. Malyukin

Institute for Scintillation Materials, STC "Institute for Single Crystals", National Academy of Sciences of Ukraine, 60 Lenin Ave., 61001 Kharkiv, Ukraine

Received January 22, 2014

Processes of excitation energy migration in $EuMgB_5O_{10}$ and EuP_3O_9 quasi-one-dimensional matrices have been investigated by means of steady-state and time-resolved luminescence spectroscopy. It was shown that the patterns of energy migration in these materials are sufficiently different — while for $EuMgB_5O_{10}$ the most effective energy transport takes place at room temperature via $^5D_0 \rightarrow {}^7F_1$ transitions of Eu^{3+} ion, for EuP_3O_9 energy transfer is more effective at low temperatures and mediated by Eu^{3+}–O^{2-} charge transfer states. The difference in energy transport processes can be explained taking into account the peculiarities of phonon subsystem for borate and phosphate matrices.

Методом стационарной и разрешенной во времени спектроскопии исследованы процессы миграции энергии возбуждения в квазиодномерных матрицах $EuMgB_5O_{10}$ и EuP_3O_9. Показано, что механизмы миграции энергии в этих матрицах существенно различны — в то время, как для $EuMgB_5O_{10}$ наиболее эффективный транспорт имеет место при комнатной температуре и происходит при участии $^5D_0 \rightarrow {}^7F_1$ переходов иона Eu^{3+}, для EuP_3O_9 перенос энергии наиболее эффективен при низких температурах и обусловлен Eu^{3+}–O^{2-} переходами с переносом заряда. Различие в процессах миграции энергии может быть объяснено особенностями фононной подсистемы боратной и фосфатной матриц.

Особливості транспорту енергії у квазіодновимірних матрицях $EuMgB_5O_{10}$ та EuP_3O_9. *Н.В.Кононець, В.В.Семінько, П.О.Максимчук, І.І.Беспалова, А.О.Масалов, Ю.В Малюкін.*

Методом стаціонарної і дозволеної у часі спектроскопії досліджено процеси міграції енергії збудження у квазіодновимірних матрицях $EuMgB_5O_{10}$ і EuP_3O_9. Показано, що механізми міграції енергії в цих матрицях істотно різні — у той час, як для $EuMgB_5O_{10}$ найбільш ефективний транспорт має місце при кімнатній температурі і відбувається за участю $^5D_0 \rightarrow {}^7F_1$ переходів іона Eu^{3+}, для EuP_3O_9 перенесення енергії найбільш ефективне при низьких температурах і обумовлене Eu^{3+}–O^{2-} переходами з переносом заряду. Різниця у процесах міграції енергії може бути пояснена особливостями фононної підсистеми боратної і фосфатної матриць.

1. Introduction

Effective transport of excitation energy to luminescent centers is a key for design of high performance optical materials. As was shown recently, in low dimensional systems (one- and two-dimensional) the processes of energy migration are sufficiently modified as compared to three dimensional systems. In a set of papers the change of migration character for low dimensional systems was shown [1–6]. For instance, in [1] it was shown that for one-dimensional systems the time dependence of quenching function

$P(t)=\ln(I/I_0) + t/\tau_0$ is changed from $P(t) \sim t$ (as observed for three-dimensional structures) to $P(t) \sim t^{0.33}$.

Recently, one and two dimensional energy transport was observed for such structures as $EuAl_3B_4O_{12}$ [2], $NaEuTiO_4$ [3], EuO_2SO_4 [4], EuOCl [5] and Sr_2CeO_4 [6]. The processes of one-dimensional excitation transport also were investigated for $REMgB_5O_{10}$ (RE=Eu, Tb) and EuP_3O_9 bulk materials at intra-center excitation [7]. In this paper we present the results obtained for $EuMgB_5O_{10}$ and EuP_3O_9 powders excited at 266 nm (excitation in Eu^{3+}–O^{2-} charge transfer band) and 532 nm (intra-center excitation). As will be shown in our paper the processes of energy migration in these systems strongly depends as on the type of excitation, so on the type of crystal lattice. Such a behavior is determined by crucial role of phonon subsystem peculiarities in energy relaxation processes.

2. Experimental methods

$EuMgB_5O_{10}$ and $LaMgB_5O_{10}:Eu^{3+}$ (0.01 at.%) powders were synthesized by co-precipitation method. Europium (III) oxide (Eu_2O_3), lanthanum (III) oxide (La_2O_3), magnesium oxide (MgO) and boron oxide (B_2O_3) were dissolved in required proportions in nitric acid. Aqueous ammonia solution was added to resulting transparent solution until precipitation of metal hydroxides (pH ~8–9). Then the precipitate was heat-treated for 8 h at 80°C, 250°C and 500°C. The final annealing was carried out at 750°C for 8 h.

EuP_3O_9 and $LaP_3O_9:Eu^{3+}$ (0.01 at.%) powders were synthesized by solid state method. Europium (III) oxide (Eu_2O_3), lanthanum (III) oxide (La_2O_3), and ammonium dihydrophosphate ($NH_4H_2PO_4$) taken in required proportions were milled in agate mortar, then heated to 600°C with heating speed of 50°C/h and maintained at this temperature for 10 h. Then the powder again was grounded in an agate mortar, and annealed at 1000°C for 15 h.

The purity of crystal phase was controlled by XRD. The luminescence decay was taken using the time-correlated single-photon counting (TCSPC) technique [8] at 300 K and 77 K. The $^5D_0$ luminescence was excited by YAG:Nd laser (λ_{exc} = 266 nm and 532 nm).

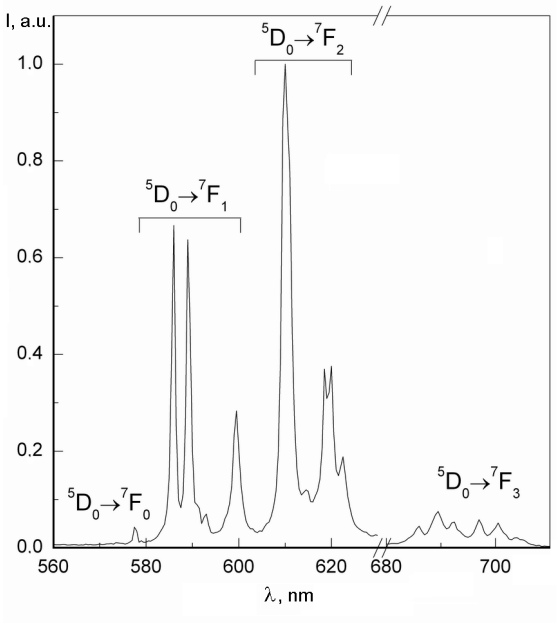

Fig. 1. Luminescence spectrum of $LaMgB_5O_{10}:Eu^{3+}$ (0.01 at.%). T = 300 K.

3. Results and discussion

3.1. One- and multistep energy transfer in $EuMgB_5O_{10}$

Crystal structure of bulk $REMgB_5O_{10}$ crystals was described in [9]. As was shown in [9], $REMgB_5O_{10}$ consists of edge-sharing REO_{10} polyhedra arranged into one-dimensional chains. The average distance between rare-earth ions in the chain is ~4 Å, while the distance between different chains is much more — about 6.4 Å. Such structure allows to suppose the effective one-dimensional migration of excitation energy through the chains and sufficiently less effective — between the chains. To determine the relative contribution of energy migration to electronic excitation relaxation processes for these materials, $LaMgB_5O_{10}$ crystal matrices with 0.01 at.% and 100 at.% of Eu^{3+} were obtained.

The luminescence spectrum for $LaMgB_5O_{10}:Eu^{3+}$ (0.01 at.%) powder excited by YAG:Nd laser (λ_{exc} = 266 nm) is shown in the Fig. 1. The spectrum consists of characteristic Eu^{3+} $^5D_0 \rightarrow {}^7F_J$ (J = 0, 1, 2, 3) transitions. The local symmetry of rare-earth center in $REMgB_5O_{10}$ is rather low (monoclinic, space group — $P2_1/c$), so complete splitting of Eu^{3+} $^5D_0 \rightarrow {}^7F_J$ transitions is observed. The $^5D_0 \rightarrow {}^7F_0$ transition is absolutely forbidden (as $0 \rightarrow 0$ transition), so its intensity is relatively low as

compared with $^5D_0 \rightarrow {}^7F_1$ and $^5D_0 \rightarrow {}^7F_2$ intensity but it still can be observed in the spectrum due to low symmetry of cationic centre.

$^5D_0 \rightarrow {}^7F_2$ decay curves for $LaMgB_5O_{10}:Eu^{3+}$ at 77 K and 300 K (λ_{exc} = 266 nm) are shown in Fig. 2a. Decay curves for $LaMgB_5O_{10}:Eu^{3+}$ are monoexponential as for 77 K, so for 300 K with decay time τ_0 = 2.7 ms and do not depend on the temperature. So in this case we can exclude one- or multistep energy transfer between doped ions and consider τ_0 as intrinsic decay time of isolated Eu^{3+} luminescent center in $LaMgB_5O_{10}$ crystal lattice.

For investigation of energy migration peculiarities between Eu^{3+} centers in $REMgB_5O_{10}$ lattice $EuMgB_5O_{10}$ were obtained. Luminescence spectrum of $EuMgB_5O_{10}$ at 266 nm excitation coincide with spectrum of $LaMgB_5O_{10}:Eu^{3+}$ and is not shown here.

$^5D_0 \rightarrow {}^7F_2$ decay curves for $EuMgB_5O_{10}$ at 77 K and 300 K are shown in the Fig. 2b (λ_{exc} = 266 nm). Both curves are non-exponential, but 300 K decay curve exhibit more pronounced deviation from monoexponential decay law. Deviation from monoexponential decay law usually is associated with one- or multistep energy transfer from optical centres to quenching centres that can be as intentionally introduced, so of intrinsic nature. In [1] was shown that in the case of one-dimensional energy migration the long-time part of decay curve must follow the law $I = I_0\exp(-t/\tau_0 - Bt^{1/3})$. Approximation of 77 K and 300 K decay curves by this law is shown in the upper inset of Fig. 2b. This approximation confirm the one-dimensional type of energy migration and allows to determine energy migration rate B that increases from 1.5 $ms^{-1/3}$ to 3.4 $ms^{-1/3}$ at temperature increase from 77 K to 300 K.

The initial parts of both decay curves show sufficient deviation from $\sim t^{1/3}$ law. Such deviation can be explained taking into account an impact of one-step energy transfer between Eu^{3+} ion and adjacent energy acceptor. For dipole-dipole mechanism of energy transfer the decay law takes the form: $I = I_0\exp(-t/\tau_0 - \gamma t^{1/2})$ [10, 11]. Approximation of initial parts of 77 K and 300 K decay curves by $\sim t^{1/2}$ law allows to determine that forster rate constant γ increases from 0.75 $ms^{-1/2}$ at 77 K to 2 $ms^{-1/2}$ at 300 K (Fig. 2b, lower inset).

So, for $EuMgB_5O_{10}$ the processes of both one- and multistep energy transfer are temperature-dependent and occur via dipole-dipole interaction. As will be shown in section 3.3, such mechanism of energy migration is possible due to high value of Debye energy in borate matrices.

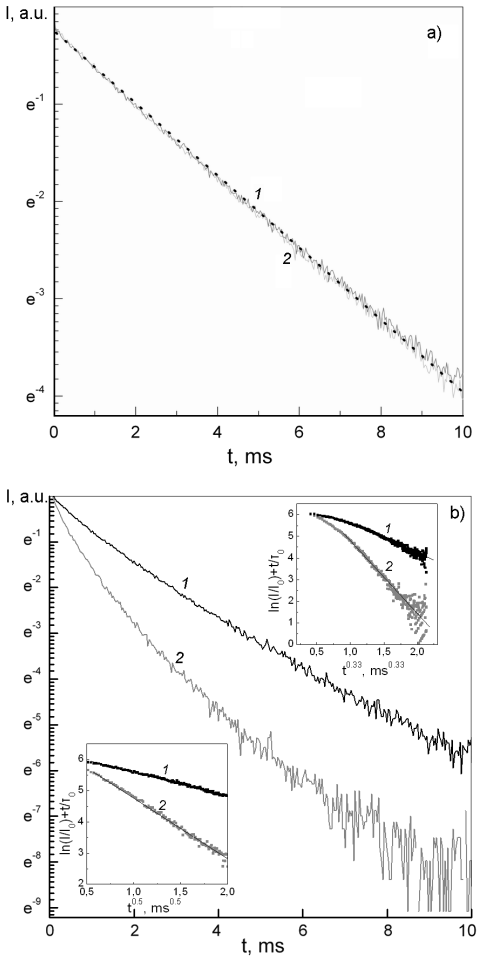

Fig. 2. $^5D_0 \rightarrow {}^7F_2$ decay curves of (a) $LaMgB_5O_{10}:Eu^{3+}$ (0.01 at.%) and (b) $EuMgB_5O_{10}$. λ_{exc} = 266 nm, *1* — 77 K, *2* — 300 K. In the insets: upper — curves 1 and 2 in $\{\ln(I/I_0) + t/\tau_0, t^{0.33}\}$ coordinates, lower — initial parts of curves *1* and *2* in $\{\ln(I/I_0) + t/\tau_0, t^{0.5}\}$ coordinates.

3.2. One- and multistep energy transfer in EuP_3O_9

Crystal structure of bulk REP_3O_9 (where RE=Ce...Gd) crystals was described in [12]. The local symmetry of RE center is *C*222 (orthorhombic). REP_3O_9 structure consists of zigzag chains of rare-earth ions arranged along to *c* axis. The average distance between these chains is about 7.3 Å and between RE ions in the same chain — 4.2 Å. So, the structure of rare-earth sublattice in

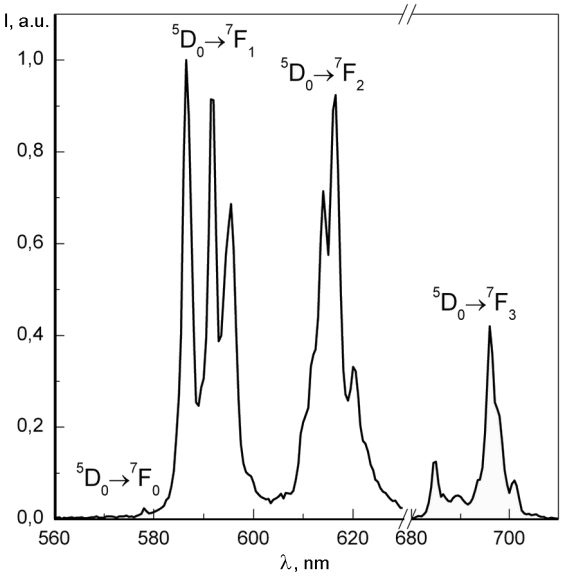

Fig. 3. Luminescence spectrum of $LaP_3O_9:Eu^{3+}$ (0.01 at.%). T = 300 K.

REP_3O_9 is quite similar to structure of rare-earth sublattice in $REMgB_5O_{10}$ and can be treated as quasi-one-dimensional. Likewise, the effective one-dimensional energy transport can be also expected for these lattice.

To determine the impact of energy migration to excitation energy relaxation processes for this lattice, LaP_3O_9 with 0.01 at.% and 100 at.% of Eu^{3+} were obtained. The luminescence spectrum for $LaP_3O_9:Eu^{3+}$ (0.01 at.%) excited by YAG:Nd laser (λ_{exc} = 266 nm) is shown in the Fig. 3. It consists of characteristic Eu^{3+} $^5D_0 \rightarrow {}^7F_J$ (J = 0, 1, 2, 3) transitions. The local symmetry of rare-earth center in REP_3O_9 structure is higher than in $REMgB_5O_{10}$ one (orthorhombic and monoclinic, respectively), so the splitting of Eu^{3+} $^5D_0 \rightarrow {}^7F_J$ transitions for LaP_3O_9 is less complete than for $LaMgB_5O_{10}$. Also the ratio of $^5D_0 \rightarrow {}^7F_2$ transition intensity relative to $^5D_0 \rightarrow {}^7F_1$ one is less for EuP_3O_9 than for $EuMgB_5O_{10}$ due to higher degree of local symmetry of the centre.

$^5D_0 \rightarrow {}^7F_2$ decay curves for $LaP_3O_9:Eu^{3+}$ at 77 K and 300 K (λ_{exc} = 266 nm) are shown in Fig. 4a. Decay curve for $LaP_3O_9:Eu^{3+}$ at 300 K is monoexponential with decay time ~4 ms. Decay curve for $LaP_3O_9:Eu^{3+}$ at 77 K consists of two stages: initial non-monoexponential stage and subsequent exponential decay (~4 ms). At such a low concentration processes of multistep energy migration between Eu^{3+} ions can be

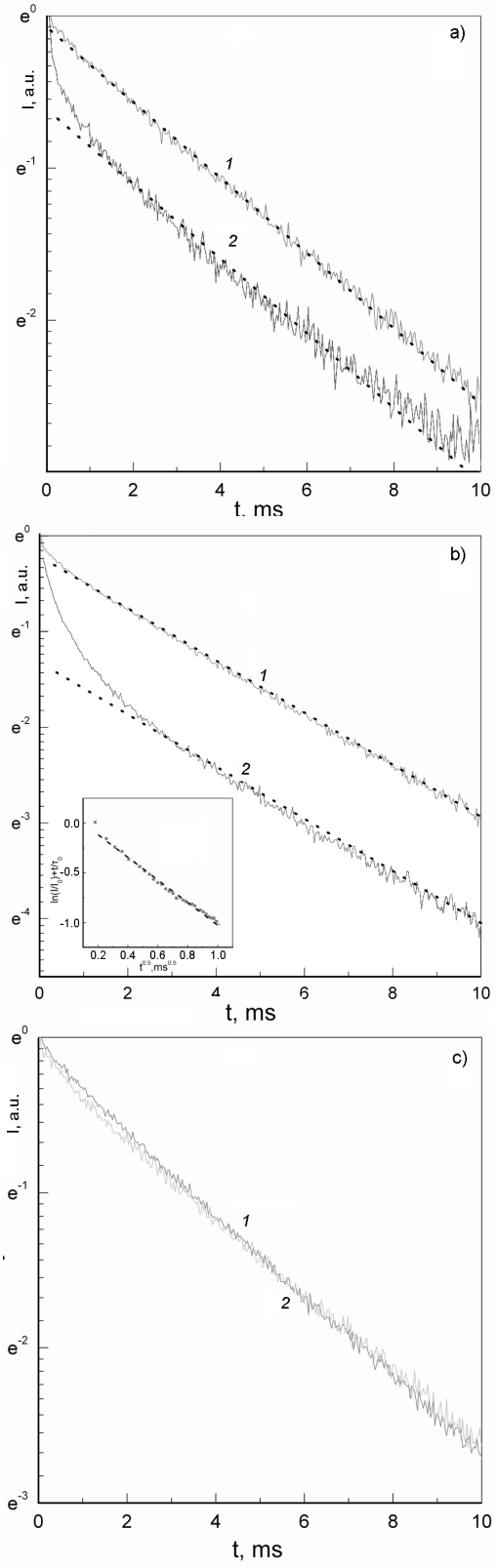

Fig. 4. $^5D_0 \rightarrow {}^7F_2$ decay curves of: (a) $LaP_3O_9:Eu^{3+}$ (0.01 at.%) and $EuMgB_5O_{10}$ at λ_{exc} = 266 nm (b) and λ_{exc} = 532 nm (c). *1* — 300 K, *2* — 77 K. In the inset — decay curve (b) in $\{\ln(I/I_0) + t/\tau_0,\ t^{0.5}\}$ coordinates.

neglected, so decay time of 4 ms can be associated with intrinsic decay of Eu^{3+} centers. Nature of 77 K decay curve deviation from monoexponential law at initial stage will be clarified lower.

For investigation of energy migration between Eu^{3+} centers in REP_3O_9 lattice EuP_3O_9 powders were obtained. Luminescence spectrum of EuP_3O_9 at 266 nm excitation coincide with spectrum of LaP_3O_9:Eu^{3+} and is not shown here.

$^5D_0 \rightarrow {}^7F_2$ decay curves for EuP_3O_9 at 77 K and 300 K are shown in the Fig. 4b (λ_{exc} = 266 nm). Decay curve for EuP_3O_9 at 300 K is monoexponential with $\tau \sim 4$ ms, while at 77 K the curve shows a sufficient deviation from monoexponential decay law at initial stage which is more pronounced that for LaP_3O_9:Eu^{3+}. The decay time of 4 ms is equal to intrinsic decay time τ_0 of $^5D_0 \rightarrow {}^7F_2$ Eu^{3+} transition in LaP_3O_9:Eu^{3+}, while the initial deviation of 77 K curve must be associated with some one-step or multistep energy transfer that occurs preferentially at low temperatures.

Such temperature dependence of energy transfer is rather unusual for rare-earth ions. As a rule, inhomogeneous broadening leads to slight difference between positions of $4f$ energy levels of adjacent RE ions, so to overcome the difference between these levels participation of phonons is required. So at temperature increase processes of energy transfer become more effective.

Excitation spectra for all $^5D_0 \rightarrow {}^7F_J$ (J = 0, 1, 2, 3) consist of the wide band with maximum at about 250 nm and width of ~3000 cm^{-1} that can be ascribed to Eu^{3+}–O^{2-} CT transition [13] and set of $4f$–$4f$ transitions (Fig. 5). Obtained temperature behavior of decay curves can be explained if we suppose that energy transfer at 266 nm excitation (excitation through CT band) occurs not between $4f$ states of Eu^{3+} ions but directly between charge-transfer (CT) states. The width of Eu^{3+}–O^{2-} CT band is ~3000 cm^{-1} (while for intra-center $4f$–$4f$ transitions ~10–20 cm^{-1}), so no phonons required to overcome the inhomogeneous broadening. Moreover, at room temperature CT states show very fast relaxation to lower levels [14]. Analysis of decay curve (Fig. 4b, inset) has shown that initial part is well approximated by $\sim t^{0.5}$ law, so forster mechanism of energy transfer can be supposed. To prove this supposition, the intra-center excitation of $^5D_0$ transition was provided (λ_{exc} = 532 nm) (Fig. 4c). As can be

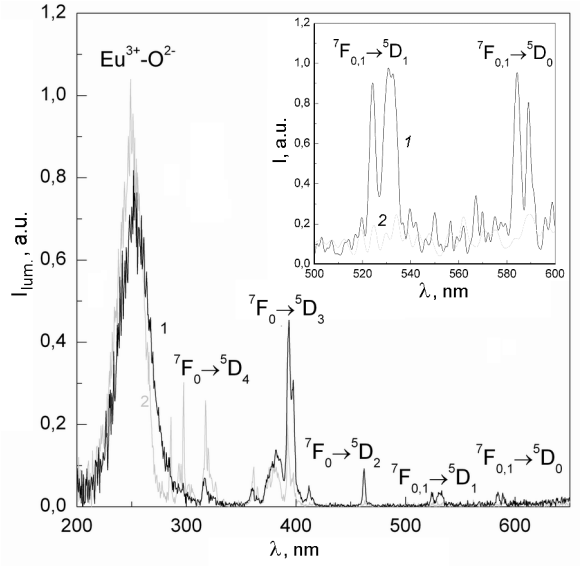

Fig. 5. Excitation spectra of $EuMgB_5O_{10}$ (*1*) and EuP_3O_9 (*2*), λ_{reg} = 696 nm. In the inset — the same spectra in the range from 500 to 600 nm.

seen from the figure, for intra-center excitation both decay curves are monoexponential and no deviation is observed. So it can be concluded that energy transfer between Eu^{3+} ions or Eu^{3+} ion and adjacent uencher of defect nature occurs in EuP_3O_9 via Eu^{3+}–O^{2-} CT band, while migration via $4f$ levels of Eu^{3+} ions is absent.

3.3. Comparison of energy migration mechanisms in $EuMgB_5O_{10}$ and EuP_3O_9

The experimental results obtained for $EuMgB_5O_{10}$ and EuP_3O_9 demonstrate clearly that in spite of very similar structure the processes of energy transfer in these matrices are sufficiently different. While for $EuMgB_5O_{10}$ energy migration occurs by dipole-dipole interaction between $4f$–$4f$ transitions of Eu^{3+} ions, for EuP_3O_9 energy transfer is occurs via CT states. To clarify why dipole-dipole interaction cannot provide an effective pathway for Eu^{3+} $^5D_0$ excitation migration, the features of thermal population of $^7F_1$ level for $EuMgB_5O_{10}$ and EuP_3O_9 were investigated. It was shown previously [15] that energy transfer between Eu^{3+} ions is rather ineffective when it takes place via $^5D_0 \rightarrow {}^7F_0$ transitions (due to absolutely forbidden nature of $0 \rightarrow 0$ transitions). However, when $^7F_1$ level is thermally populated, migration can occur via $^5D_0 \rightarrow {}^7F_1$ transitions and becomes rather more effective.

The excitation spectra of $EuMgB_5O_{10}$ and EuP_3O_9 (λ_{reg} = 696 nm) are shown in Fig. 5. The spectra are quite similar and consist of wide band with maximum at about 250 nm (which can be assigned to Eu^{3+}–O^{2-} charge transfer (CT)) and set of narrow lines between 300 and 600 nm ($4f$–$4f$ transitions). The same spectra in the range of 500–600 nm are shown in the inset. In the spectra of $EuMgB_5O_{10}$ besides number of transitions from $^7F_0$ level there are also two bands that can be assigned to $^7F_1 \rightarrow {}^5D_1$ and $^7F_1 \rightarrow {}^5D_0$ transitions. These bands are absent in the spectra of EuP_3O_9, so it can be supposed that thermal population of $^7F_1$ level is considerably lower for EuP_3O_9 than for $EuMgB_5O_{10}$. Difference between thermal population levels for EuP_3O_9 than for $EuMgB_5O_{10}$ can be explained by lower values of Debye energy for REP_3O_9 lattice (~1200 cm^{-1}) than for $REMgB_5O_{10}$ one (more than 1400 cm^{-1}) [7, 16].

The difference in Debye energy can explain absence of energy transfer via CT states for $EuMgB_5O_{10}$ as well. Increase of phonon energy increases the probability of thermal relaxation of CT state thus drastically decreasing the probability of radiative relaxation or energy transfer to another center. So this concept allows to explain the difference between energy transfer processes in $EuMgB_5O_{10}$ and EuP_3O_9 matrices.

4. Conclusions

In the paper processes of energy migration in $EuMgB_5O_{10}$ and EuP_3O_9 matrices were investigated. It was shown that in spite the fact that the energy migration process is quasi-one-dimensional in both these matrices, the specific mechanisms of energy transfer are completely different — namely, for $EuMgB_5O_{10}$ it occurs via $^5D_0 \rightarrow {}^7F_1$ transitions and its efficiency is determined by thermal population of $^7F_1$ level, while for EuP_3O_9 the main channel of energy delocalization is interaction between Eu^{3+}–O^{2-} CT states. The difference between energy transfer mechanisms in $EuMgB_5O_{10}$ and EuP_3O_9 is explained by differences in phonon subsystems for these materials.

References

1. B.Movaghar, C.W.Sauer, D.Wurtz, *J. Stat. Phys.*, **27**, 473 (1982).
2. F.Kellendonk, G.Blasse, *J. Chem. Phys.*, **75**, 561 (1981).
3. P.A.M.Berdowski, G.Blasse, *J. Luminescence*, **29**, 243 (1984).
4. P.A.M.Berdowski, R.Van Mens, G.Blasse, *J. Luminescence*, **33**, 147 (1985).
5. P.A.M.Berdowski, J.Van Herk, G.Blasse, *J. Luminescence*, **34**, 9 (1985).
6. O.Viagin, A.Masalov, I.Ganina, Yu.Malyukin, *Opt. Mat.*, **31**, 1808 (2009).
7. M.Buijs, G.Blasse, *J. Luminescence*, **5**, 263 (1986).
8. D.O'Connor, Time-correlated Single Photon Counting, Academic Press, New York (1984).
9. B.Saubat, M.Vlasse, C. Fouassier, *J. Sol. St. Chem.*, **34**, 271 (1980).
10. Th.Forster, *Ann. Phys.*, **437**, 55 (1948).
11. J.R Lakowicz, Principles of Fluorescence Spectroscopy, Springer, New York (2006).
12. H.Y-P.Hong, *Acta Cryst. B*, **30**, 468 (1974).
13. D.Wang, Y.Wang, L.Wang, *J. Electrochem. Soc.*, **154**, J32 (2007).
14. G.Blasse, B.C.Grabmaier, Luminescent Materials, Springer-Verlag, Berlin (1994).
15. C.Fouassier, B.Saubat, P.Hagenmuller, *J. Luminescence*, **23**, 405 (1983).
16. C.T.Dinh, P.V.Huong, R.Olazcuaga, C. Fouassier, *J. Opt. Adv. Mat.*, **2**, 159 (2000).